Cement and Concrete Composites 129 (2022) 104473

Contents lists available at ScienceDirect

Cement and Concrete Composites

journal homepage: www.elsevier.com/locate/cemconcomp

Centrifugally sprayed Engineered Cementitious Composites: Rheology, mechanics, and structural retrofit for concrete pipes

He Zhu, Duo Zhang, Victor C. Li *

Department of Civil and Environmental Engineering, University of Michigan, Ann Arbor, MI, 48109, USA

ARTICLE INFO

Keywords:
Concrete pipe
Engineered cementitious composites (ECC)
Centrifugal spray
Rehabilitation
Rheology

ABSTRACT

Current trenchless rehabilitation techniques for deteriorated concrete pipelines have limitations in field operation, pipeline geometry and size, durability, and structural retrofit. In this research, an innovative technology utilizing centrifugally sprayed ECC (CS ECC) to retrofit cracked concrete pipes is established. Rheology is engineered by hydroxypropyl methylcellulose for viscosity enhancement, citric acid for rheology evolution retardation, and hybrid synthetic fibers for flowability control. CS ECC is demonstrated capable of building up to 50 mm thickness on both vertical and horizontal concrete pipes, with reachable diameters over 300–900 mm. A 25 mm CS ECC (5.7 MPa-tensile strength and 5.3%-ductility) lining enhances the cracked concrete pipe by 2.2 times in load capacity and by 1.5 times in deformation capacity. Combining the advantages of mechanical and leak-proof performance, low cost, fast construction, self-healing ability, and expansive coupling with host pipe, the developed CS ECC holds promises in rehabilitating concrete pipelines, tunnels, and culverts.

1. Introduction

Concrete is one of the most widely used materials for pipelines conveying drinking and wastewater [1,2]. More than 2.1 million km of wastewater pipelines and 3.5 million km of drinking water pipeline have been installed in the US [3]. For developing countries, new pipelines are being constructed at high speed, e.g. China is expected to expand new drainage pipelines at a rate of 10% annually [1]. Due to its brittle nature, concrete is vulnerable to cracks, which can be induced by imposed deformations and loadings [4]. Poor bedding, excessive external loading/displacement, and temperature fluctuation could cause cracking. Once cracked, seepage could remove the surrounding soil of the pipeline and further aggravate the cracking. Moreover, the corrosive liquids and bacteria in sewer exacerbate the deterioration of concrete pipelines, reducing the service life or even causing pipe incidents. According to the ASCE report [3], a water main break occurs every 2 min in the US. Tremendous opportunities exist for renovating concrete pipelines to address current and future needs.

Compared to the excavation methods, trenchless (no-dig) restoration methods have the advantages of being cost-effective, less disturbance to the ground (traffic and residents), environmentally friendly, and fast construction [1,5,6]. Cure-in-place pipe (CIPP), and fiber-reinforced polymer (FRP) can structurally strengthen the concrete pipe under internal pressure, however, contribute less to external-load resistance due to the low stiffness of the CIPP and FRP liner. Sliplining (SL) can achieve a structural effect under both external and internal loads by inserting a new pipe and by grouting between the host and the new pipe. However, the structural enhancement depends on the thickness of grout, leading to a significant reduction of hydraulic capacity by the SL method [7]. Sprayed cementitious materials have the advantages of low cost and ease of application compared to CIPP, FRP, and SL methods. The structural performance of deteriorated pipes can be restored by increasing the thickness of cement/mortar/concrete liner. Similar to the SL method, the increased liner thickness reduces the diameter of the flow section and consequently decreases the hydraulic capacity of the pipeline. Moreover, the cementitious material liner is prone to cracking, compromising the strengthening effect. Hence, a trenchless rehabilitation method possessing the capability of repairing and retrofitting concrete pipelines without the above-mentioned limitations is needed.

To overcome the brittle shortcoming of concrete, Engineered Cementitious Composites (ECC) have been invented by deliberate design of matrix, matrix-fiber interface, and fiber reinforcement, exhibiting high tensile ductility (usually>3%) and controlled micro-cracks (e.g. below 100 μm in width). ECC has been successfully demonstrated on repairing and retrofitting structures, especially on dams, tunnels, culverts, and irrigation channels [8–12], which have many similarities to

* Corresponding author.
E-mail addresses: zhuhe@umich.edu (H. Zhu), duzhang@umich.edu (D. Zhang), vcli@umich.edu (V.C. Li).

https://doi.org/10.1016/j.cemconcomp.2022.104473
Received 18 October 2021; Received in revised form 7 January 2022; Accepted 2 March 2022
Available online 3 March 2022

concrete pipelines, such as underground application, wet service conditions, and concrete-ECC bonding. Moreover, ECC has the ability of autogenous healing due to the intrinsically small crack width. Although cracks may be generated in an ECC liner, the microcracks can be expected to undergo self-healing in the typical wet environment of pipelines [13–16]. Further, expansive ECC [17,18] has been developed that autogenously exerts pressure when confined by the host pipe. The expansive ECC not only reduces the shrinkage cracking risk but also enhances the integral coupling between the ECC liner and the repaired pipe. These advantages suggest the viability of repairing and retrofitting concrete pipes with ECC.

ECC can be processed by mold-cast, self-consolidating, extrusion (3D-Print), and spraying methods [9,10,19,20]. However, the present ECC processing method shows limitations on pipe application, which has limited space for manual spraying or a considerable high cost for mold-casting. A centrifugal spraying method has been developed for applying conventional shotcrete or fiber-reinforced concrete on pipe repair [21–23]. In contrast with shotcrete that utilizes compressed air to atomize the concrete/mortar into small particles, the centrifugal spraying method employs a spin-caster rotating at a high rate, the centrifugal force renders the mortar into small spraying particles. However, the relatively high dosage of fibers (2% volume addition) increases the challenge of applying the centrifugal spraying method for ECC. To develop the innovative centrifugally sprayed ECC (CS ECC) for repairing/retrofitting pipelines, issues such as the rheology design, mechanical performance, and pipe-ECC structural performance must be carefully investigated.

ECC sprayability requires the control of the rheology of the paste (before fiber addition) and that of the ECC (with fibers). Moderate viscosity (>6 Pa s [24]) of the paste is necessary to facilitate fiber dispersion during the mixing process in order to obtain a robust tensile strain-hardening performance [24] of ECC composite. In addition, a two-stage rheology evolution is proposed for sprayable ECC. A relatively large initial flowability is suitable for pump and spray operation followed by a rapid increase of viscosity/decrease of flowability for thickness build-up [10,25]. To enhance the build-up ability, calcium aluminate cement [25] or calcium sulphoaluminate cement (CSA) [10] is utilized due to its rapid hardening characteristic. Besides the chemical additives (such as hydroxypropyl methylcellulose and water reducer [25]), additions of fibers increase the yield stress and viscosity significantly, depending on fiber type and quantity [20,26,27]. Despite comprehensive studies on rheology control of ECC for normal applications [24,28–30], the rheology design method for CS ECC has not been reported in the literature. Requirements include the breaking-up of the fresh material into particles under centrifugal force. Meanwhile, fiber-matrix segregation should be avoided during spraying. Finally, the CS ECC needs to be built up to a desired thickness on the pipe wall (both above-head and horizontally) without dripping.

In addition to the fresh properties, the mechanical performance after centrifugal spraying, especially the tensile ductility, is critical for the ultimate performance of the repaired pipe. Two factors may affect the tensile ductility of the CS ECC, i.e., fiber orientation and flaw distribution. The centrifugal spraying process could change fiber orientations, resulting in anisotropy of tensile performance. Macro flaws are observed in conventional sprayable ECC, of which the tensile strength/ductility is lower than that of mold cast specimens [8,10,31]. Further at the structure level, the retrofit effect of the concrete pipe repaired with CS ECC remains to be studied.

The objective of this study is to develop an innovative technology utilizing the centrifugally sprayed ECC (CS ECC) to retrofit cracked concrete pipes. The new processing method of CS ECC involves the engineering/control of material rheology, centrifugal spraying test, and uniaxial tensile test. Finally, the retrofit effect of concrete pipe using CS ECC is demonstrated per ASTM C76-20 [32].

2. Experimental program

2.1. Materials and test protocol

Based on the previous developed ECC which has been demonstrated sprayable and expansive [10,17,18], a composited cement including Type I ordinary Portland cement (OPC), calcium sulphoaluminate cement (CSA), metakaolin (MK), and limestone powder (LS) was employed to develop the centrifugal sprayed ECC (CS ECC). The CSA was 160 kg/m^3 to obtain a self-stressing effect that autogenously applies expansive pressure onto the pipe when curing [10,17]. MK and LS were utilized for the dual benefits of material greenness and rheology control suitable for sprayable ECC [10,17,18]. Crumb rubber (CR, 40–80 mesh) was utilized as artificial flaws for inducing saturated cracks of ECC [33]. Table 1 lists the ECC proportion of dry ingredients, where the water was 356 kg/m^3 (0.27 times of binder weight) to obtain a 40 MPa of compressive strength, comparable to the minimum strength requirement of Class V concrete pipe (41 MPa/6000 psi) per ASTM C76-20 [32]. More details of the materials (Table 1) regarding the particle size, chemical compositions, and SEM pictures have been reported in previous studies [16,17].

Hydroxypropyl methylcellulose (HPMC from ACROS Organic) was adopted to modulate the viscosity of the ECC paste. Kim et al. [34] suggest that when HPMC content is larger than 1‰ of binder weight, non-adsorbing HPMC molecules will increase significantly. Moreover, excess HPMC introduces more entrained air and reduces the strength [24]. Therefore, 1‰ binder weight of HPMC was set as an upper limit and three HPMC dosages (0‰/0.5‰/1‰ weight of binder) were designed, denoted as H0, H5, and H10, respectively.

Besides the initial viscosity influenced by HPMC, the rheology evolution (or hardening rate) affects the spraying process significantly. Since the rapid hardening of CSA cement shortens the time window for spraying, citric acid (anhydrous, 99% purity, from ACROS Organics) was utilized for tuning the setting time of the sprayable ECC, which has been demonstrated feasible for CSA based ECC [30]. As proposed by Zhu et al. [30], 0‰/2‰/4‰ binder weight of citric acid was used and denoted as C0/C2/C4. The Mix ID and test protocol are listed in Table 2.

While PVA fiber is widely utilized for moderate tensile strength (4–6 MPa) and ductility ECC (3%–5%) [9], hydrophobic polyethylene (PE) fibers can be used for high tensile strength (>6 MPa) and high ductility ECC (>6%) [35]. Besides the mechanical performance, fresh properties of ECC (yield stress, viscosity, and spread diameter) are influenced by fibers, such as fiber type, diameter, length, and volume [20,28,29]. Both PVA and PE fibers are selected for tailoring the fresh and hardened properties of centrifugal sprayed ECC (details can be found in Section 3.1.4 and 3.2). 2% volume of PVA fibers, 2% volume of PE fibers, the hybrid of 1% volume PVA and 1% volume PE were prepared for developing centrifugally sprayed ECC, named PVA ECC, PE ECC, and Hybrid ECC. Table 3 lists the technical specifications of PVA and PE fibers.

2.2. Sample preparations

Dry ingredients (OPC, CSA, MK, LS, FA, sand, CR, and HPMC) were pre-mixed for 5 min using a Hobart HL300 Planetary Mixer (28.4-L of volume). Then water associated with HRWR and citric acid (if used) was added and further mixed for 5 min at 100 rpm. Subsequently, the rheology test and flow table test were performed on the fresh paste. To prepare the ECC samples, fibers were added to the fresh pastes and

Table 1
Mix proportion of ECC composition (kg/m^3).

OPC	CSA	MK	LS	FA	Sand	CR	HRWR[a]
310	160	180	90	580	400	30	15

[a] High-range water reducer (Master Glenium 7920 from BASF).

Table 2
Test protocol of the ECC and pastes.

Mix ID	HPMC/binder (‰)	Citric acid/binder (‰)	Rheology test	Flow table test	Uniaxial tension test	Centrifugal spray test
H0 paste	0	2	X	X	–	–
H5 paste	0.5	2	X	X	–	–
H10 paste	1	2	X	X	–	–
C0 paste/ECC	0.5	0	X	X	–	–
C2 paste/ECC	0.5	2	X	X	–	–
C4 paste/ECC	0.5	4	X	X	–	–
PVA ECC	0.5	2	X	X	X	–
Hybrid ECC	0.5	2	X	X	X	X
PE ECC	0.5	2	X	X	X	–

Note: The notation "X" means the test was conducted, while "-" represents that tests were not performed.

Table 3
Technical specifications of PVA and PE fibers.

Fiber type	Density (kg/m^3)	Tensile strength (MPa)	Young's modulus (GPa)	Elongation (%)	Diameter (μm)	Length (mm)
PVA[a]	1300	1600	42.8	6	39	8
PE	970	3000	100	2–3	20	12

[a] PVA fiber with 1.2% weight of oil coating.

mixed at 200 rpm for an additional 5 min. The whole process of sample preparation can be found in Fig. 1. After obtaining a homogeneous fiber dispersion, rheology, flow table, uniaxial tension, and centrifugal spraying tests were performed. The uniaxial tensile specimens were prepared with dogbone-shaped molds (Fig. 2). To examine the effect of curing condition on composite properties, both air curing (20 ± 3 °C, 40 ± 5% RH) and water curing (20 ± 3 °C) for 28d were adopted for the dogbone-shaped specimens. Uniaxial tension tests follow the protocol in Table 2, where each test included 3 specimens per batch. Two linear variable displacement transducers (LVDT) attached to the opposite sides of the dogbone-shaped specimens (Fig. 2) were used to measure the tensile deformation.

2.3. Fresh properties test

A mini-slump cone (diameter $d_0 = 10$ cm) per ASTM C1437 [36] was used for the flow table test. After lifting the mini-cone, the pastes spread on the flow table, and the spread diameter was measured once the pastes come to a rest. Due to the addition of fiber, ECC tends to retain its shape under self-weight [20], so the flow table was dropped 25 times in 15 s per ASTM C1437 [36]. The maximum spread diameter (d_1) and the diameter perpendicular to d_1 (marked as d_2) (Fig. 3) were recorded. A deformability index (D) is calculated based on the spread diameter (Eq. (1)) and adopted as a criterion for the sprayability of ECC [10,20,25].

$$\mathrm{D} = \frac{(d_1 \times d_2) - d_0^2}{d_0^2} \tag{1}$$

Besides the flow table test, an ICAR Plus Rheometer (Fig. 4) was employed to characterize the rheology parameters. The measured torque (T) and rotational speed (N) can be fitted on a regressed curve as

$$T = G + HN + CN^2 \tag{2}$$

where G, H, C are the fitting parameter of the T-N relation. According to the Modified-Bingham model (M − B), the yield stress (τ) and viscosity (μ) can be derived by Reiner–Riwlin equation [37]:

$$\tau = \frac{\left(\frac{1}{R_i^2} - \frac{1}{R_o^2}\right)}{4\pi h \ln\left(\frac{R_o}{R_i}\right)} G \tag{3}$$

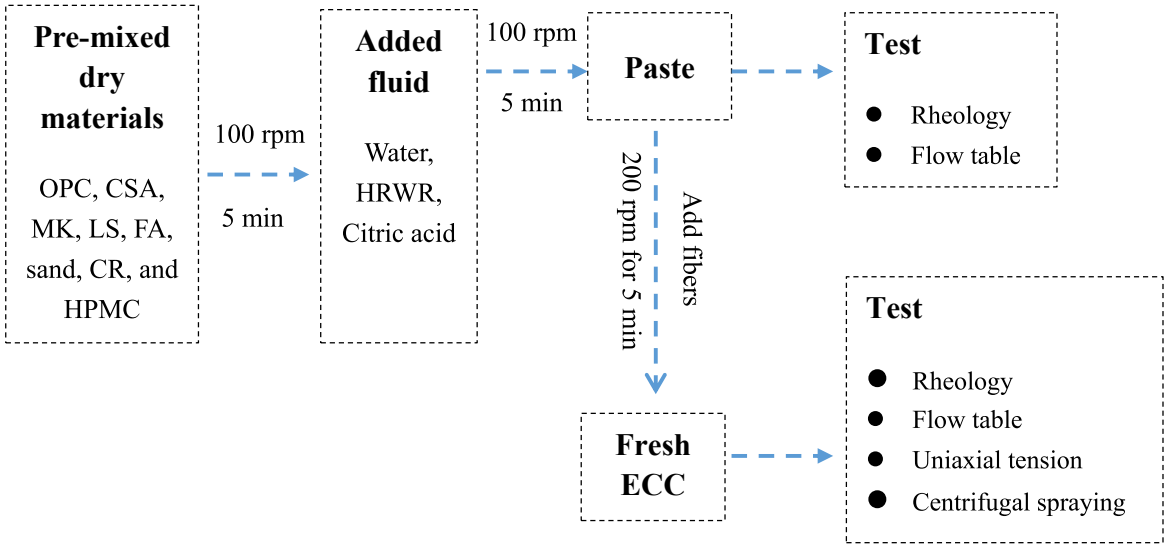

Fig. 1. The mixing procedure of ECC/paste samples.

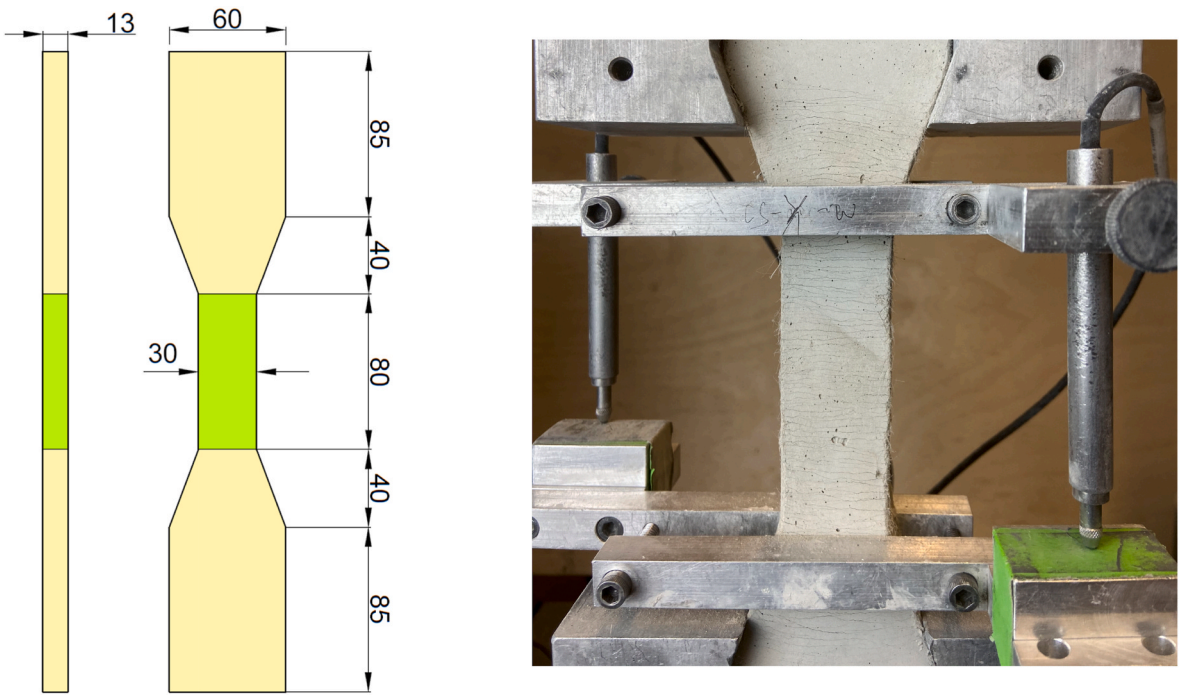

Fig. 2. The dimension of the dogbone-shaped specimen. (Unit: mm).

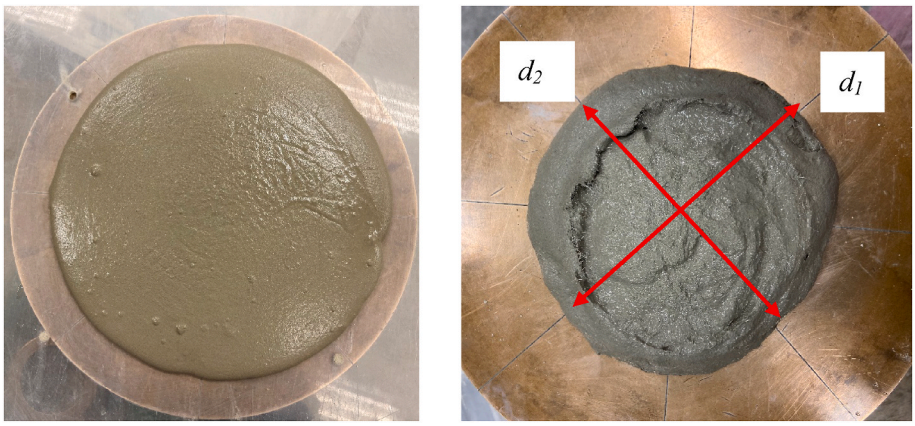

Fig. 3. Flow table test of paste (left) and ECC (right).

$$\mu = \frac{\left(\frac{1}{R_i^2} - \frac{1}{R_o^2}\right)}{8\pi^2 h} H \tag{4}$$

where R_i and R_o are the vane radius and container radius, which are 63.5 mm and 75 mm, respectively. h is the height of the vane height (127 mm). The reason that the M − B model was selected rather than other models is detailed in Section 3.1.1.

Once mixing of the fresh paste/ECC (Fig. 1) was completed, the time was set as zero-time. Both the flow table test and rheological test were conducted at 5 min, 30 min, 60 min, 90 min, and 120 min to monitor the evolution of fresh properties.

2.4. Centrifugal spray tests

With deliberate designs of both rheological and hardened properties (Section 3.1 and *3.2*), Hybrid ECC (Table 2) was utilized for pipe centrifugal spray test. As shown in Fig. 5, the ready-mixed ECC is conveyed by a material pump, then fed into the spin-sprayer which is driven by compressed air. In contrast to the conventional shotcrete or sprayable ECC that the material was atomized by the high-pressure air, the compressed air in a centrifugal pump does not contact ECC but drives the spinner at high rotating speed, leading to the ECC being sprayed out radially from the disk (Fig. 5 (b)) due to the centrifugal force. The ECC was sprayed circumferentially and built on the pipe wall layer-by-layer (Fig. 5). After desired thickness, the spinner was lifted by the frame along the pipe axis, so that the ECC can build up seamlessly along with the longitudinal directions. Generally, higher rotational speed impels a larger centrifugal force, resulting in high kinetic energy of the sprayed ECC and ejected to a further distance. Although the reach-diameter of the centrifugal sprayed ECC can be controlled by varying the air pressure/volume, this study intends to demonstrate the feasibility of CS ECC for retrofitting pipes, rather than establishing the relationship between compressed air and reach-diameter of CS ECC.

After some trial tests, the air pressure was fixed at approximately 689 kPa (100 psi) with a volume of 30 CFM during the spray test. A reinforced concrete pipe (RC pipe) of 300 mm inner diameter was adopted for both vertical and horizontal spraying tests (Fig. 5(a–b)).

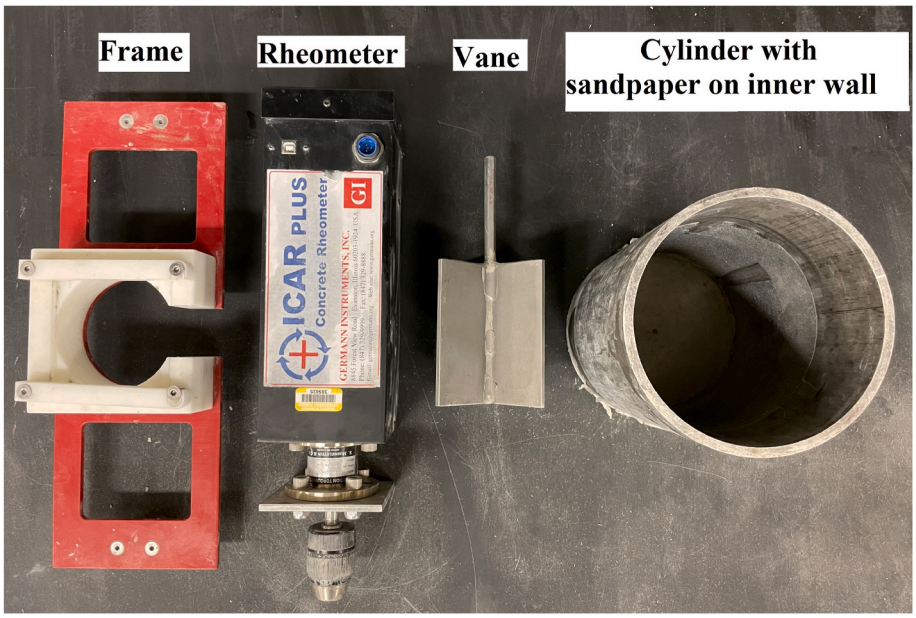

Fig. 4. ICAR plus rheometer.

Moreover, a larger reach-diameter (900 mm) of CS ECC was demonstrated using a metal pipe; 300–900 mm diameter can meet the general applications of RC pipe for wastewater [1,38]. During the centrifugal test, dogbone molds were placed against the metal pipe inside wall, where specimens were positioned in both circumferential (CS-C) and longitudinal directions (CS-L), for evaluation of the effect of centrifugal spray process on the expected anisotropic tensile performance of CS ECC. Similar to the 300-mm concrete pipe, the dogbone-molds were also continuously filled in both circumferential and longitudinal directions using the centrifugal sprayer (Fig. 5c).

2.5. Pipe retrofit test

RC pipe sections with 300-mm inner diameter, 450-mm outer diameter, and 400-mm height were obtained from Northern Concrete Pipe Inc. (MI, USA), which meets the Class V Reinforced Concrete per ASTM C76-20 [32]. All six pipe sections were cut from a 2500 mm-length RC pipe to assure consistent quality. One RC pipe was crushed to failure (marked as Pipe_Ref) with a three-edge bearing test method (Fig. 6) per ASTM C497M − 19 [39]. Five RC pipes were also loaded to generate cracks. However, these pipes were unloaded after the first peak when the RC pipes were already cracked. The five pre-cracked RC pipes were subsequently repaired by CS ECC method with different built-up layer thicknesses, i.e., 25 mm, 28 mm, 32 mm, 38 mm, and 50 mm. Once the target thickness is attained, the spraying repaired pipes were vertically placed in air (20 ± 3 °C, 40 ± 5% RH) and cured for 28 days. Then the repaired RC pipes were retested by the three-edge bearing test method to examine the retrofit effect of CS ECC.

3. Experimental results and discussions

3.1. Fresh properties

3.1.1. Rheology model selection

The representative torque-speed relationship (Fig. 7) exhibits more like a non-linear distribution, rather than a linear model. Although the linear Bingham model can fit the data with a correlation coefficient of 0.97, the calculated dynamic yield stress using the Bingham model is −44.7 Pa, which should be a positive value to be physically meaningful. In contrast, the Modified-Bingham (M − B) model can describe the non-linear relation of torque and speed, where all the correlation coefficients of curve fitting in this study are larger than 0.99. Therefore, the M − B model is selected to fit the non-linear rheology parameters for both pastes (without fibers) and ECC (with fibers) compositions.

The paste rheology reveals a shear-thickening effect, where the (apparent) viscosity increases with increasing shear rate [40]. Both the order-disorder theory and clustering theory have been proposed to explain the shear-thickening behavior [41,42]. The order-disorder theory deems that the particles are in ordered layers at a low shear rate and shift to a disordered state at high shear rate. The disordered particles exhibit a “jamming effect”, resulting in increased viscosity [43]. Although the mechanism is not completely understood, the low water/binder ratio and admixtures (HPMC and metakaolin) have been observed to enhance the shear-thickening tendency [40,41,44], supporting the shear-thickening enhancement of the composition used in this study.

The shear-thickening enhancement of paste has an additional benefit for dispersing the fibers, especially for PE fibers. Due to the smaller diameter of PE fiber (20 μm) compared to PVA fiber (39 μm), the quantity of PE fiber is 3.8 times of PVA fiber for the same length and volume dosage [1]. In addition to the hydrophobic surface, PE fibers are more difficult to disperse than PVA fibers. The higher viscosity of the ECC pastes at a high shear rate favors improved fiber dispersion, where the mixing speed of ECC is usually about 200 rpm. Further, this advantage can also be applied for polypropylene fibers, which is more challenging as it has a smaller diameter (12 μm) and has 10.6 times of fiber quantity compared to PVA fibers [16].

With the addition of fibers, the shear-thickening of pastes converts to a shear-thinning rheological character in ECC. Because coarse sandpaper is placed on the inner wall of the container, no apparent sliding is observed during the tests. Structural breakdown and fiber alignment by high-speed shear flow are plausible reasons for the reduced viscosity with increased shear rate, revealed as a shear-thinning effect [45,46]. During the centrifugal spray process, the material viscosity decreased under a high rotational speed, leading to a reduction of material cohesion. Consequently, the ECC material is easier to be sprayed into small particles under a high centrifugal force, facilitating the spraying process of ECC. In addition, once the ECC particles are projected onto the substrate, the microparticles start to build up. Under the static condition, the yield stress/viscosity of ECC reverses to increase again. The recovered cohesion boosts the thickness build-up without sloughing or dripping.

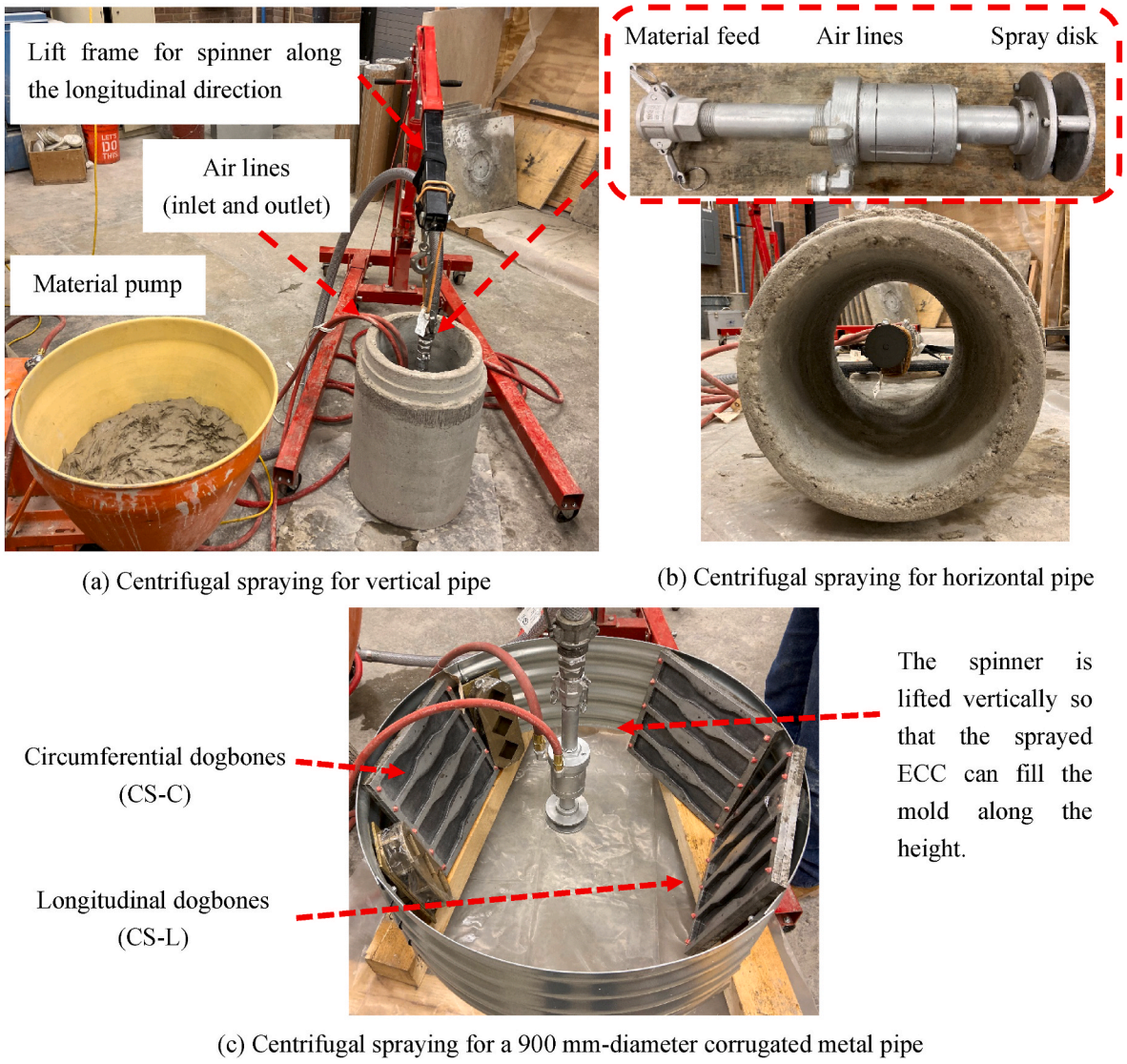

Fig. 5. Demonstration of centrifugally sprayed pipe with different directions and diameters.

3.1.2. HPMC effect

Hydroxypropyl methylcellulose (HPMC) noticeably increases the yield stress and viscosity of ECC pastes, depending on the HPMC dosage. Negligible improvement of yield stress is observed between H0 and H5 (Fig. 8 (a)), however, the yield stress is significantly enhanced as the HPMC dosage increases to 0.10% (H10). In contrast, both H5 and H10 boost the plastic viscosity considerably, e.g., the initial viscosity increases from 0.5 Pa s (H0) to 27.6 Pa s (H10) (Fig. 8 (b)). The viscosity of pastes increases at a similar rate with time evolution (at least before 90min), indicating the robustness of HPMC effects on viscosity enhancement with time.

Similar to the rheological parameters, the spread diameter of both pastes and ECC decreased with the addition of HPMC (Fig. 9). The initial free spread diameter of H10 diminishes to 178 mm compared to 349 mm of H0. The loss of fluidity caused by the addition of HPMC has been widely observed [44,47,48]. On one hand, both the HPMC and HRWR adsorb on the surface of cement grains, the competitive adsorption of HPMC weakens the repulsive force contributed by HRWR. On the other hand, HPMC polymer particles can also precipitate/adsorb/wrap on the surface of HRWR, annulling the dispersion ability of HRWR [48,49]. Further, H0 exhibits a faster decline with time than H5 and H10. This phenomenon has also been reported by Kong et al. [50]. The long polymeric chains of HPMC behave as a steric layer on the binder particle surface, physically maintaining the particles' space [9], and delaying the fluidity loss of the ECC pastes. The steric action of HPMC slows the spread diameter loss of H5/H10 with time compared to that of H0.

The deformability of Hybrid-ECC with fibers (Fig. 9 (b)) shares a similar trend with that of the ECC pastes (Fig. 9 (a)). The initial deformability of H0 is 2.0, dropping to 1.2 when 1‰ binder weight of HPMC is added. Increased viscosity has been demonstrated to facilitate fiber dispersion and increase tensile ductility [24]. However, an excess dosage of HPMC can increase the entrained air voids, decreasing the matrix strength [24,51]. Moreover, the diminished deformability increases the challenge of sprayability of ECC, where the deformability below 1.5 has been proven unsuitable for spraying with compressed air [30]. Although the optimal deformability range has not been investigated for centrifugally sprayed ECC (CS ECC), H10 is not recommended for CS ECC due to its low deformability, specifically the deformability of H10 decreases below 1.0 after 30 min. Hence, H5 is selected for CS-ECC considering the advantages of fiber dispersion and rheology modification reasons.

3.1.3. Citric acid effect

Citric acid has negligible influence on the yield stress before 60 min for the composition used in this study; however, citric acid slows the growth rate of yield stress after 60 min (Fig. 10 (a)). Plastic viscosity also

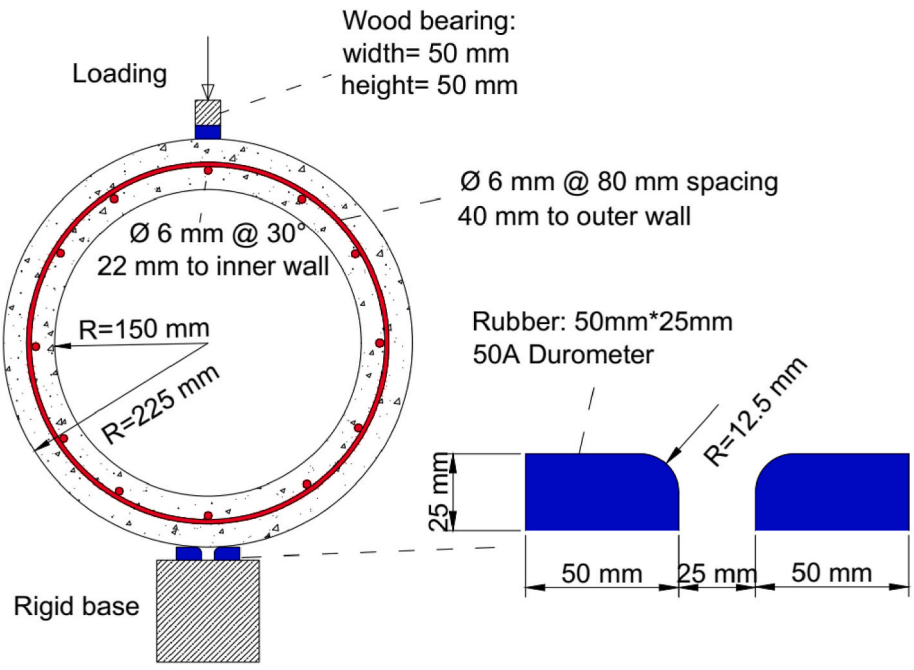

Fig. 6. Three-edge bearing test of the RC/ECC repaired pipes (400-mm height).

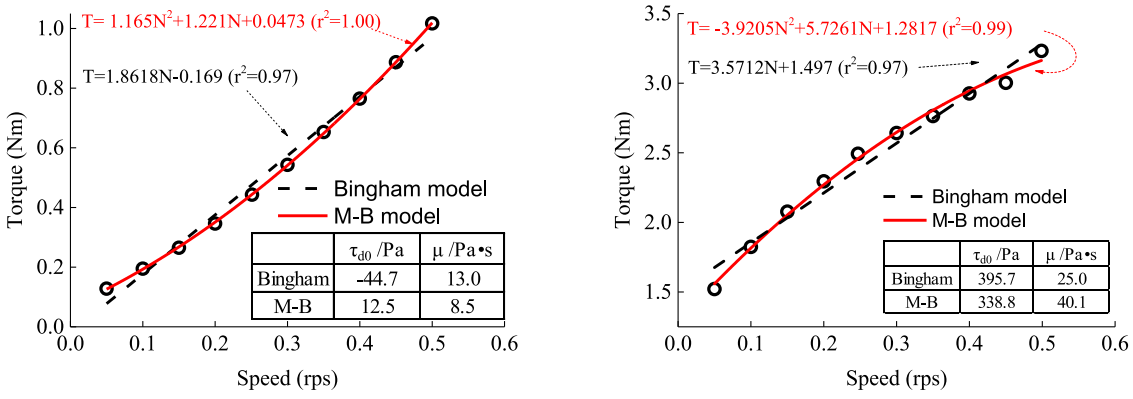

(a) Paste (shear-thickening) (b) ECC (shear-thinning)

Fig. 7. Representative torque-speed curve of H5-C2-hybrid at 5 min.

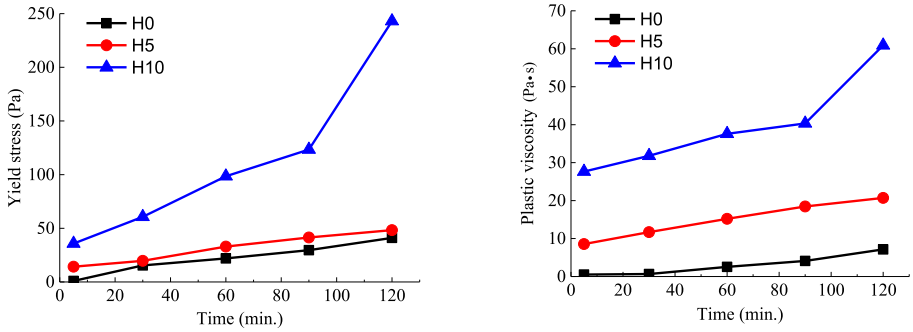

(a) Yield stress (b) Viscosity

Fig. 8. HPMC effect on the rheological parameters.

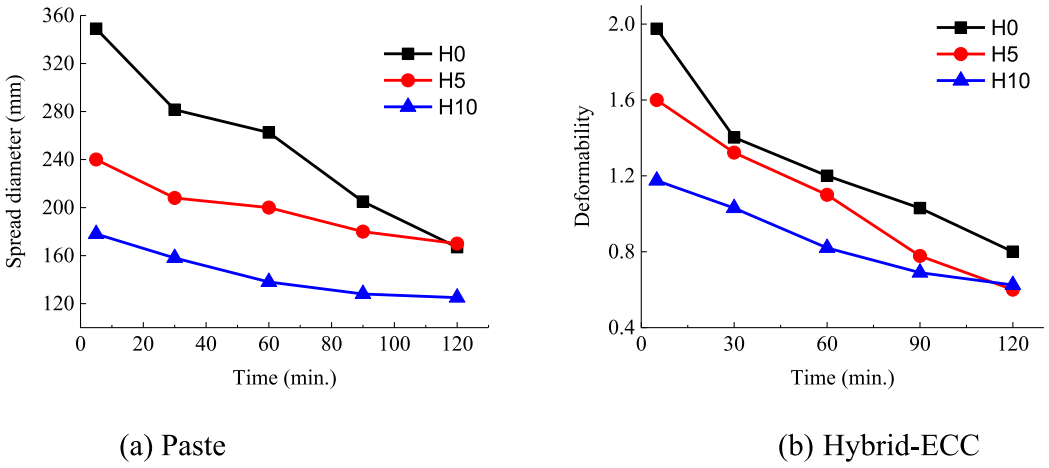

Fig. 9. HPMC effects on results of flow table tests.

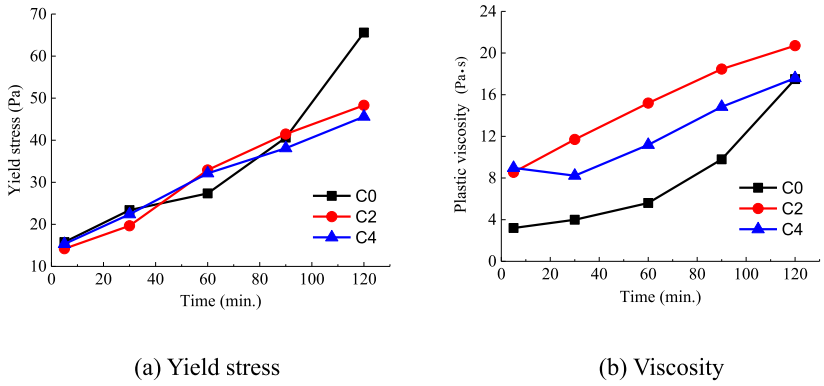

Fig. 10. Citric acid effects on rheological parameters.

exhibits a retarded increase speed after 60 min, while the initial viscosity is enhanced from 3.2 Pa s (C0) to 9.0 Pa s (C4) with the addition of citric acid (Fig. 10 (b)). Further, the flow table test (Fig. 11) also shows a decreased initial flowability accompanied by a slower decay with time when citric acid is incorporated. These findings have also been observed previously [30,52]. Similar to the HPMC effect, citric acid competes with HRWR [53] for particle adsorption, decreasing the initial viscosity/fluidity. At a later time, citric acid retards the hydration of CSA and suppresses the precipitation of ettringite, resulting in the slow growth of rheology parameters and flow loss.

Although the initial deformability of Hybrid ECC is decreased by citric acid, C2 Hybrid ECC maintains larger deformability than C0 Hybrid-ECC after 30 min. Further, C4 Hybrid ECC shows the highest deformability among C0 and C2 Hybrid-ECC at 120 min, suggesting that citric acid can effectively slow down the deformability loss with time, which is critical to maintaining the sprayability of ECC [10,30]. Moreover, if high initial fluidity is required, the compromised initial deformability can be recovered by increasing the HRWR dosage.

3.1.4. *Fiber effect*

The effect of fibers on rheology properties is more pronounced in comparison to that of HPMC and citric acid. Fig. 12 shows that the initial

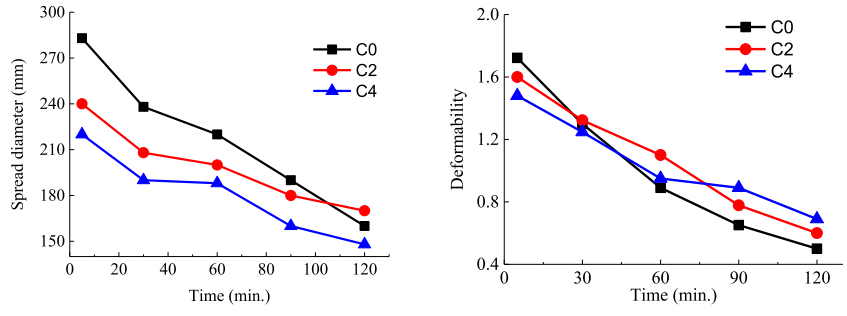

Fig. 11. Citric acid effects on flow table tests.

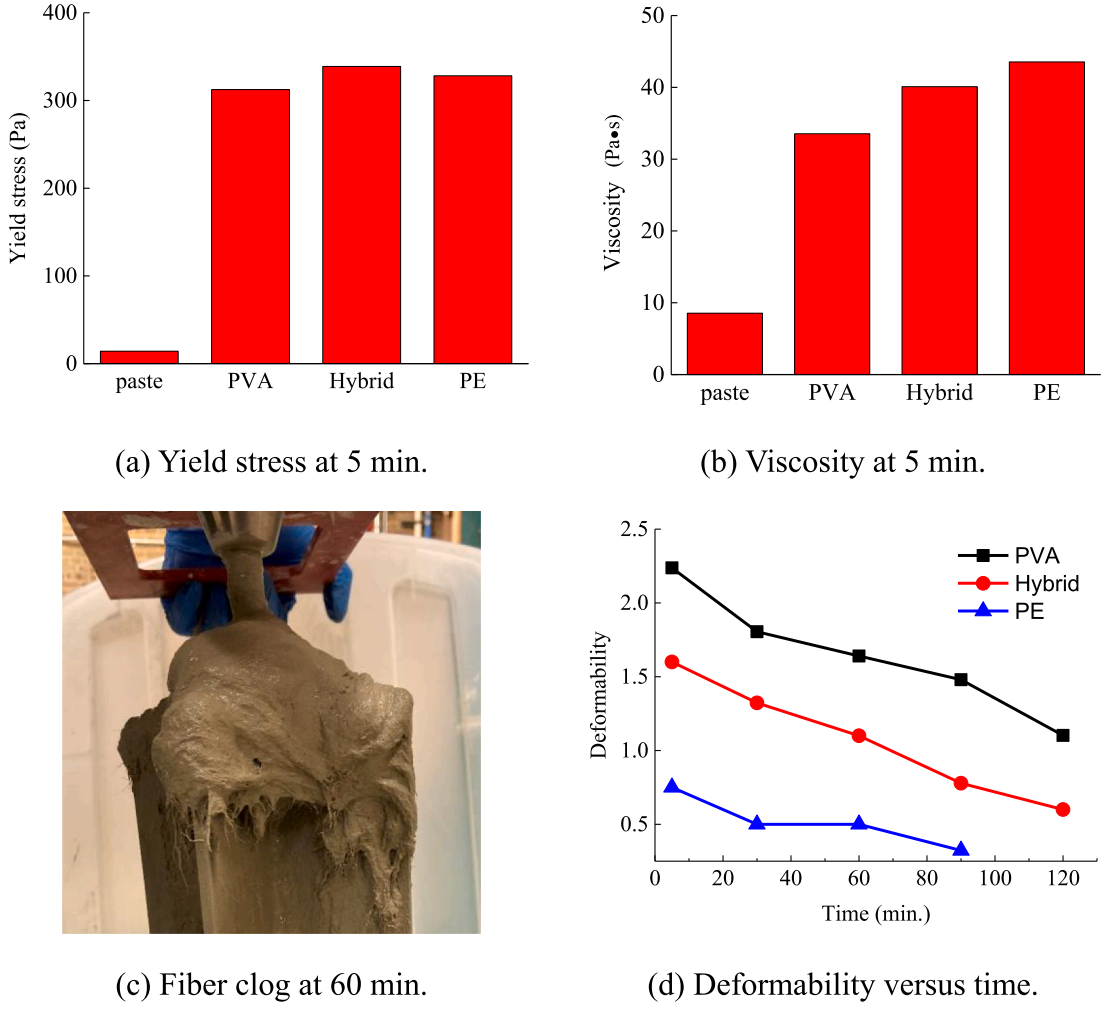

Fig. 12. Fiber effects on rheology and deformability.

dynamic yield stress varies from 14.2 Pa (paste) to more than 300 Pa (ECC). Further, the initial viscosity increases from 8.5 Pa s (paste) to 33.5 Pa s (PVA ECC), 40.1 Pa s (Hybrid ECC), and 43.5 Pa s (PE ECC), respectively. Synthetic fibers tend to deform and entangle fiber-matrix under shear, blocking the movement of particles and increasing the viscosity [49]. In addition, PE fibers have a greater influence on increased viscosity than PVA fibers, while the effect of PE/PVA hybrid fibers is somewhere in between. Although Zhang et al. [54] find that hydrophilic fiber (PVA) leads to a worse fluidity than hydrophobic fibers (PE here), the effect of fiber diameter was ignored in that study. As proposed by Grünewald [46], the fiber length/diameter ratio has a stronger impact on the viscosity. PE fibers have a smaller diameter (20 μm), leading to a larger length/diameter ratio of 600 compared to that of PVA fiber (200), accounting for the increased viscosity of PE ECC.

Due to the considerable initial yield stress and viscosity, the ECC material behaves more rigid later, due to the suppression of the HRWR/HPMC effectiveness and to further hydration. The increased rigidity invalidates the rheology test, with clogging of fibers under the effect of rotation. The clogged fiber-matrix can't be treated as homogeneous flow, as shown in Fig. 12 (c), resulting in the inapplicability of the rheology model (M − B model). In addition, fibers are prone to migrate towards the low shear-rate zone, i.e., towards the outside wall of the rheometer, and this migration can be aggravated with time [49]. Therefore, the rheology tests of ECC are only conducted at 5 min after the end of mixing without considering the time evolution. However, fibers maintain dispersion uniformity in the pump with a plug flow behavior [55]. The robustness of fiber dispersion or mechanical properties has been established in those pump conveyed ECC, such as sprayed ECC [10,30] and 3D printed ECC [20,56].

The deformability is also influenced noticeably by fiber type (Fig. 12 (d)). The initial deformability of PVA ECC is 2.2. This value drops to 1.6 for PE/PVA hybrid ECC and 0.8 for PE ECC. The low deformability (0.5) of PE ECC at 30 min imposes a challenge of pumping and spraying. Although the initial deformability can be restored by increasing the HRWR amount, the paste will be very flowable (i.e. low viscosity), which is detrimental for fiber dispersion during mixing, and further impairs the tensile ductility of ECC. Therefore, PE ECC is not utilized for centrifugal spraying tests.

3.1.5. *Summary of rheology design*

Among the investigated factors, HPMC mainly increases the viscosity of paste, which facilitates the fiber dispersion for ECC. However, excess HPMC also decreases the deformability of ECC, imposing the challenge of sprayability of ECC. Therefore, moderate dosage of HPMC (H5) is preferred. In contrast to the viscosity modification action of HPMC, citric acid primarily controls the rheology evolution with time. i.e., controls the time window for spraying. Fibers are the dominant factor affecting the fresh properties of ECC. Since clogged fibers increase the challenge of measuring the rheological parameters, the flow table remains the most practical tool to evaluate the sprayability of ECC. The

deformability index D between 1.0 and 2.2 is proposed for centrifugal spraying. For D higher than 2.2, the built-up thickness of ECC is limited to below 25 mm [10]. For D less than 1.0, the sprayability function of ECC is lost.

3.2. Uniaxial tensile properties

The results of uniaxial tensile tests show that PE ECC has a higher ultimate tensile strength and ductility than PVA ECC regardless of air curing or water curing. The ultimate tensile strength of air-cured PE ECC is 7.9 MPa at 28d, compared to 4.5 MPa of PVA ECC. Further, water curing increases the tensile strength to 8.8 MPa and 6.2 MPa for PE ECC and PVA ECC, respectively. Although water curing has been reported to exhibit an adverse effect on tensile strain capacity due to the enhanced matrix strength [57], this side effect is not observed for the compositions of PVA ECC, PE ECC, and Hybrid ECC (Table 4) in this study. As demonstrated, the first crack strength related to the matrix increased insignificantly (Fig. 13).

PE/PVA hybrid ECC maintains 6.6 MPa of tensile strength under air curing and 8.3 MPa under water-curing, which are slightly lower than those of PE ECC. However, the tensile strain capacity (6.5–6.8%) is higher than that of PE ECC (6.2–6.4%). Due to the utilization of rapid hardening CSA cement, Hybrid ECC attains 2.1 MPa after 1d and 6.5 MPa after 7d of air curing, as well as 7.4 MPa of tensile strength under 7d of water curing, showing a comparable tensile strength to Hybrid ECC at 28 d.

Fig. 14 presents the crack patterns of ECC using different fibers and cured under air or water conditions. PVA ECC shows an unsaturated crack distribution, with 36–41 cracks within the gage length of 80 mm. PE ECC shows 89 cracks under air curing and 71 cracks under water curing with a tighter crack spacing than PVA ECC. Although 50% of PE fibers are replaced by PVA fibers, the Hybrid ECC maintains 60–83 μm of average crack width at failure, comparable to that of PE ECC at 28 d. Moreover, Hybrid ECC attains a smaller crack width of 42 μm at 1d. Water curing increases the matrix strength, resulting in a less saturated crack pattern than air curing.

Considering the balance of fiber cost and ECC performance, Hybrid ECC is chosen as the mixture for the centrifugal test, showing fast strength gain and robust tensile performance in both air and water curing conditions, advantageous for pipe rehabilitation.

3.3. Centrifugal spray test

The centrifugally sprayed ECC for vertical and horizontal pipes attains a one-time thickness of 50 mm (2 inches in Fig. 15) without dripping. The CS ECC is sprayed out from the spray disk in small particles driven by centrifugal force. The ECC particles are projected at high-speed onto the internal surface of the concrete pipe, where the ECC builds up layer by layer. During the spraying process, no-slip between ECC liner and concrete pipe is observed, indicating a good adhesion ability between the sprayed ECC and pipe surface. Moreover, the ECC itself exhibits robust cohesive ability; the ECC liner maintains its original shape without segregation until 50 mm of thickness, showing a potential for further layer thickness built-up for the vertical pipe (Fig. 15 (a)). However, the ECC liner on the top of the horizontal pipe tends to drip when the thickness exceeds 60 mm (Fig. 15 (b)), suggesting a 50 mm thickness limit for one-time application.

Another advantage of the centrifugal ECC is that no rebound is found during the build-up process ((Fig. 15). The rebound is one of the most challenging issues for conventional shotcrete, which can lead to poor material placement and material waste [58]. The rebound will cause extreme problems in pipe rehabilitation. For the vertical pipe, the rebound concrete will deposit on the bottom of the vertical pipe. Regarding the horizontal pipe, the rebound material falls directly onto the bottom of the horizontal pipe, which is hard to remove since pipelines usually have a long distance. The deposited material will block the water flow and influence the functionality of the original pipelines. The elimination of coarse aggregate is one of the main reasons for reducing the rebound [10]. Polymer fibers can dissipate the kinetic spray energy upon impact and bridge the matrix [59], which also contributes to diminishing the rebound. Finally, the deliberately designed rheology (Section 3.1) enhances the no-rebound performance of the centrifugal sprayed ECC.

The centrifugally sprayed ECC builds up 25 mm thickness on the 900 mm-diameter corrugated metal pipe (CMP) (Fig. 16), where 25 mm thickness meets most requirements of CMP repair [23]. Meanwhile, this test demonstrates that the developed CS ECC can reach a 900-mm diameter. The maximum reached diameter can be further enlarged by employing a higher air pressure and volume, which can drive the spinner at a higher rotation speed, leading to the increased kinetic energy of the sprayed particles. A maximum of 3.5 m diameter CMP has been established by centrifugal spraying technology for fiber reinforced concrete [23].

Besides the build-up thickness and reach-diameter, the centrifugally sprayed ECC offers a superior surface finish performance. Due to the small particles building up layer by layer, an even-thickness and satisfactory surface finish have been obtained without any additional surface treatment (Fig. 15). Furthermore, a rotated trowel can be applied behind the spinner to achieve a smoother surface and improved water flow capacity. The even-thickness and smooth surface show an advantage over the conventional shotcrete technology, which depends on the skill of the nozzle operator.

Finally, the centrifugally sprayed ECC technology has the ability of fast return-to-service. The centrifugal spraying method has been demonstrated to decrease the construction time to 10 days, compared to 6 weeks of robotic shotcrete [23]. Moreover, due to the utilization of CSA cement, the final setting time of developed ECC is within 3 h [10, 30]. The rapid hardening material, as well as the fast applied centrifugal spray method, is attractive to the pipeline owners since fast return-to-service reduces the overall costs and disruptions to users.

Table 4
Summary of the uniaxial tensile results.

Mixture	Air curing				Water curing			
	f_t	ε_t	Crack No.	CW	f_t	ε_t	Crack No.	CW
PVA ECC-28d	4.5	3.8	36	84	6.2	3.6	41	70
PE ECC-28d	7.9	6.4	89	57	8.8	6.2	71	70
Hybrid ECC-1d	2.1	5.1	97	42	–	–	–	–
Hybrid ECC-7d	6.5	8.4	88	76	7.4	6.2	70	71
Hybrid ECC-28d	6.6	6.8	91	60	8.3	6.5	63	83

Note: f_t and ε_t mean the ultimate tensile strength and tensile strain capacity with the unit of MPa and %, respectively. CW is the average crack width corresponding to the ultimate tensile strength, which is calculated by ε_t/Crack No.

3.4. Effect of centrifugal spraying on uniaxial tensile properties

The centrifugal spraying process affects the fiber orientation of CS ECC, showing anisotropy in the uniaxial tension test (Fig. 17 (a)). The dogbone specimen collected from the circumferential direction (CS-C) obtains 5.7 MPa of ultimate tensile strength and 5.3% tensile strain capacity (Fig. 17). In contrast, CS-L (longitudinal direction) experiences a notable reduction of tensile performance with 4.7 MPa of ultimate tensile strength and 2.2% tensile ductility. During centrifugal spraying, small ECC particles are sprayed out along the radial direction. Due to the spinning of the sprayer, sprayed particles are then projected onto the pipe internal surface along the circumferential direction, leading to a preference for circumferential fiber orientation. Since less fiber bridges the longitudinal matrix, the tensile strength and ductility are decreased.

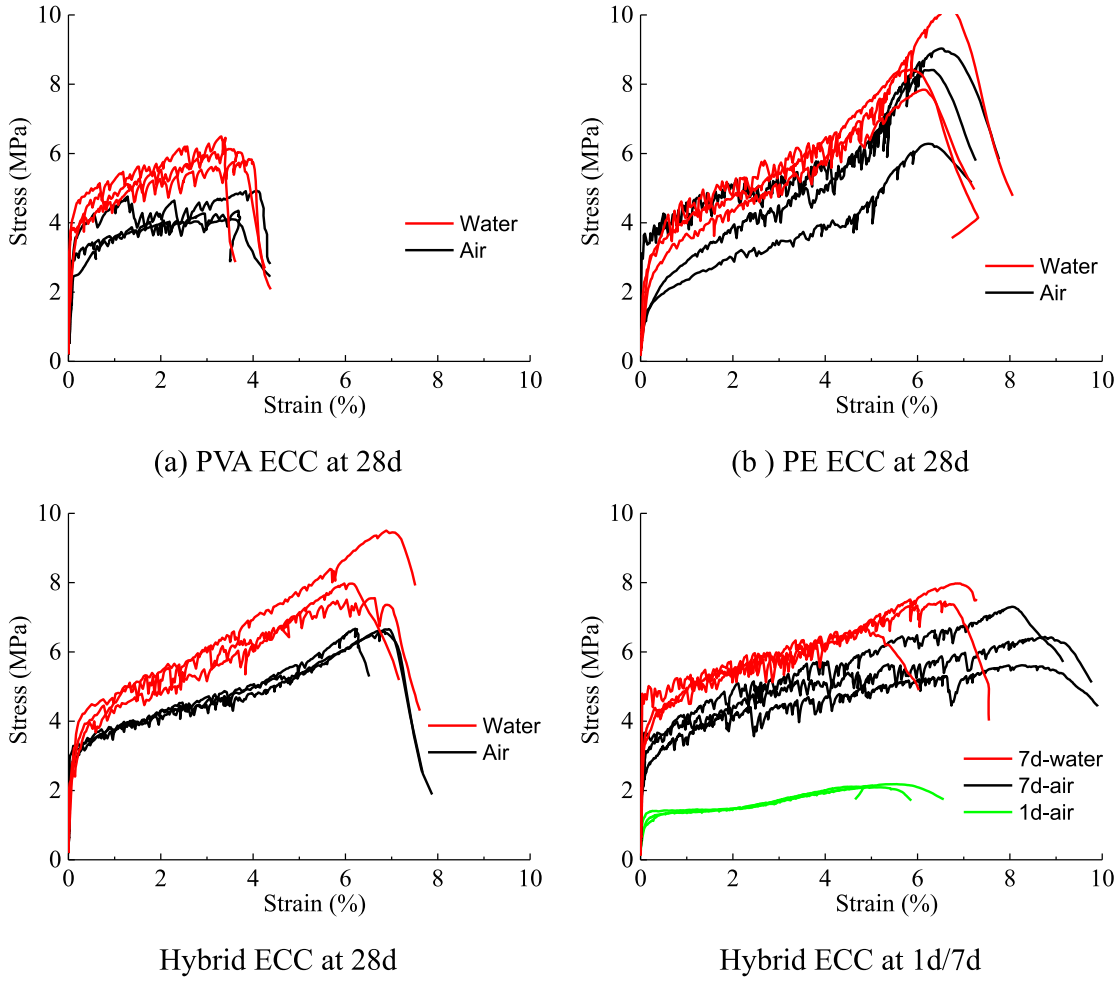

Fig. 13. Uniaxial tensile performance under water/air curing conditions.

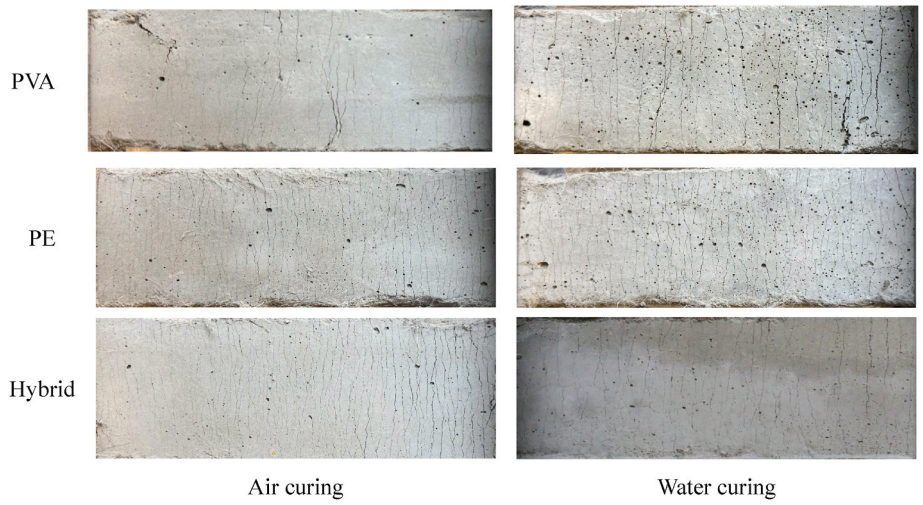

Fig. 14. The crack patterns between the gauge length (80-mm length) when dogbone specimens were tensioned to peak load at 28 d.

However, the 2.2% tensile ductility of CS-L remains more than 200 times of conventional shotcrete, while CS-C behaves more ductile with more than 500 times of ductility compared to normal concrete.

The centrifugal sprayed ECC, both CS-C and CS-L, exhibit compromised tensile properties compared to mold cast ECC (Fig. 17). Reductions of 13.6% in tensile strength and 22% in tensile ductility are observed in CS-C compared to CS-cast. While the mold cast specimens are vibrated to eliminate air-entrained flaws, the sprayed specimens may contain more air voids or macro flaws. Under uniaxial tension, the ECC specimen fails at the location with the minimum fiber bridging stress

(a) Vertical pipe (b) Horizontal pipe

Fig. 15. Centrifugal sprayed ECC for different pipe directions.

Fig. 16. Centrifugal sprayed ECC on a 900 mm-diameter corrugated metal pipe.

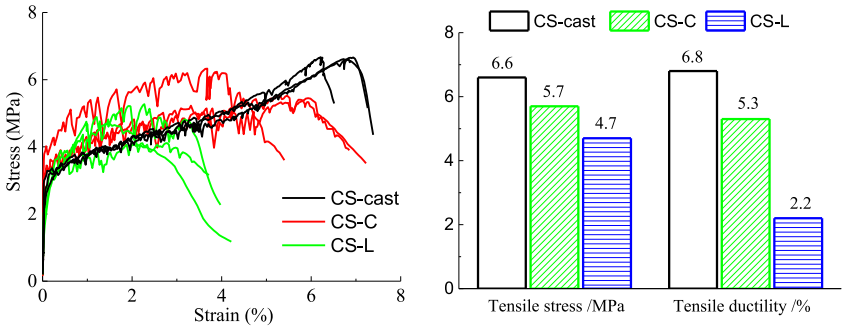

(a) Stress-strain curve of CS ECC (b) Summary of tensile strength/ductility

Fig. 17. Uniaxial tensile properties of the CS ECC.

associated with lower fiber content. The crack patterns of centrifugally sprayed ECCs (Fig. 18) show an unsaturated crack pattern but a crack width comparable to the cast specimen (Fig. 18), supporting that the centrifugal spray process generates a different flaw size distribution compared with normal casting. The less compacted ECC with macro flaws is also observed in Fig. 20. This finding is consistent with the previous research, where the sprayed ECC revealed decreased tensile strength and ductility due to flaws [8,10,31,34].

3.5. Pipe retrofit

Reinforced concrete pipes (RC pipes) may suffer significant loss of water-carrying functionality after the appearance of cracks due to the uncontrolled crack width. The reference RC pipe (Pipe_Ref in Fig. 19 (a)) shows a maximum load capacity of 50.3 kN (first peak) followed by a sudden load drop and a residual load capacity of 48.5 kN (second peak) due to the existence of reinforcing steel. The first peak corresponds to the initiation of two pairs of diametrically located cracks (Fig. 20 (a)) on the RC pipe wall. Although the cracked RC pipe retains a residual

Fig. 18. Crack patterns of CS ECC correspond to the peak load in the circumferential (CS-C) and the longitudinal (CS-L) directions.

strength, the crack width grows larger with increasing imposed deformation and leads to water leakage from the damaged pipe. As the imposed deformation further increases, the RC pipe exhibits a brittle failure into quarter sections.

CS ECC shows advantages of repair and retrofit of cracked RC pipes, demonstrating dramatic load and deformation capacity enhancements compared to RC pipes even in the virgin condition. Five RC pipes are pre-loaded to generate cracks, emulating the pre-existent cracks of pipelines. The pre-cracked pipes show 48.6 ± 2.0 kN of load capacity, indicating the consistent quality of pipe sections. After being repaired with CS ECC, both the load and deformation capacity are significantly improved, commensurate with the thickness (25–50 mm) of the CS ECC layer (Fig. 19(b–d)). The load capacity shows a linear increase with the CS ECC thickness, where 25 mm-CS ECC repaired pipe attains 110.6 kN of load capacity (2.2 times of Pipe_Ref). Moreover, 50 mm-CS ECC repaired pipe attains 326.5 kN (6.5 times of Pipe_Ref). Meanwhile, the deformation capacity is also significantly improved with 1.5–1.9 times compared to the Pipe_Ref. While 25 mm of the developed CS ECC reported here doubles the load capacity of cracked pipe, the required thickness of ECC liner can be reduced by tailoring the ECC with increased strength and ductility, such as the high strength high ductility ECC [60,61]. The tailorability of tensile strength and ductility of ECC provides opportunities for pipe owners to select low-cost (less material) high-performance retrofit solutions.

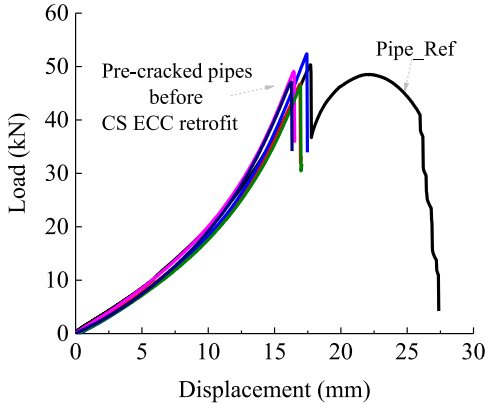

(a) Load-displacement curves of pre-cracked pipes

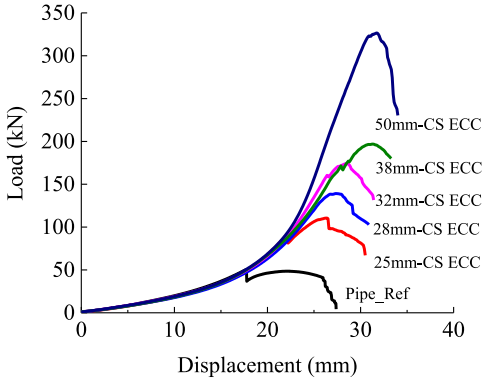

(b) Load-displacement curves of CS ECC repaired pipes

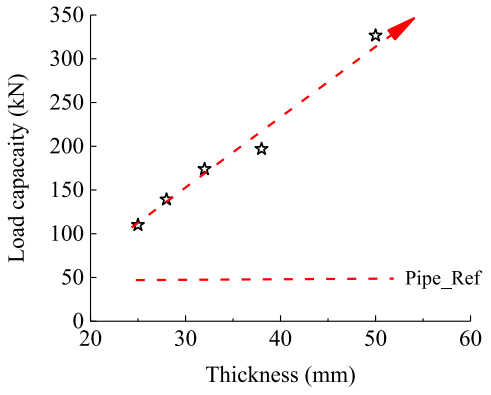

(c) Load capacity enhancement

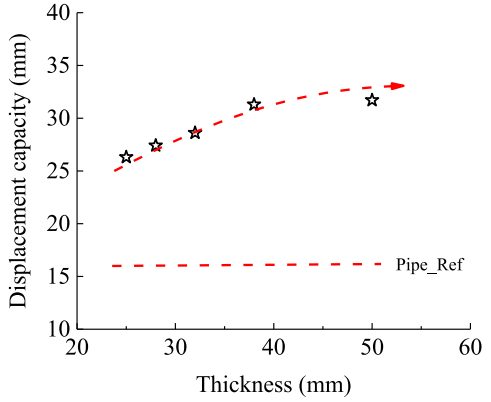

(d) Displacement capacity improvement

Fig. 19. Demonstration of pipe retrofit by CS ECC.

Fig. 20. Crack patterns of the RC-ECC pipe.

The advantages of CS ECC retrofitting concrete pipe originate from the superior crack control ability of ECC, as demonstrated in Section 3.2. Unlike the macro-cracks in concrete pipe, the ECC liner presents multiple micro-cracks (Fig. 20 (d)), suppressing the local fracture failures due to macro cracks. With increasing external load, the macro-cracks in the concrete pipe kink-propagate into the ECC liner. However, the rapidly increased crack resistance of ECC traps the kinked-crack, leading to a bifurcation along with the interface of the ECC liner and concrete pipe. Repetition of this kink-bifurcate process results in concrete debonding from the ECC liner (Fig. 20 (c)). Hence, moderate interface bonding is preferred for the ECC-concrete repaired system since excess bonding suppresses the multiple cracking of ECC while too weak bonding results in ECC-concrete debonding and limits the overall load capacity. This phenomenon was previously proposed as the kink-crack trapping mechanism for ECC-concrete systems [62,63]. At the ultimate stage, the concrete pipe spalls off, exposing the bared ECC liner with micro-crack patterns (Fig. 20 (b)). The crack patterns (Fig. 20) establish the excellent crack control ability and enable the retrofit mechanism of CS ECC with enhanced load/deformation capacity.

Some local circumferential flaws can be observed on the ECC-concrete interface (Fig. 20 (b)), implying an ECC liner not fully compacted. Although the liner compaction can be improved by further optimizing the material rheology and the axial (along pipe) travel speed of the sprayer, local flaws are inevitable during onsite centrifugal spraying, which has also been reported for conventional shotcrete/sprayed ECC [10,64]. However, since ECC is designed as a flaw-tolerant material, the CS ECC liner retains its ductile advantage and contributes to pipe retrofit even when processing defects were introduced.

Processing flaws at the liner/host pipe interface can be detrimental to conventional shotcrete as they tend to weaken the interfacial bonding of the liner and host pipe. Especially under the effect of volume deformation (e.g. shrinkage and temperature), interfacial flaws can exacerbate the delamination or debonding of the liner and host pipe. Due to the addition of CSA cement in the composition, the CS ECC possesses an intrinsic expansive property [17,18]. The expansive CS ECC applies pressure against the host pipe, thus reducing dependence on surface bonding. This deliberately designed mechanical coupling of the liner to the host pipe further diminishes the workload and cost of surface preparation of the host pipe, which is critical as well as challenging for other pipe rehabilitation methods, such as shotcrete, CIPP, and FRP rehabilitation [1].

Particularly, a centrifugal spray fiber-reinforced concrete (FRC) has been reported for repairing a cracked C50 RC pipe [21]. The repaired RC pipe, with a 57 mm tension-softening FRC lining (compressive strength of 60 MPa and tensile strength of 6 MPa), showed a compromised load capacity compared to the virgin pipe. Zhao et al. [21] suggested that the insufficient strain capacity and the poor interface bonding limited the retrofit capability of the FRC lining. In contrast, the newly developed strain-hardening CS ECC boosted the repaired concrete pipe by 2.2 times in load capacity, despite a reduced layer thickness of 25 mm and a lower strength (compressive strength of 40 MPa and tensile strength of 5.7 MPa). As discussed above, the excellent crack control ability,

self-stressing bonding, and ultra-high tensile ductility enable the developed CS ECC with the capacity of retrofitting the cracked pipe.

4. Conclusions

In this study, an innovative technology of centrifugally sprayed ECC (CS ECC) was developed to retrofit the cracked concrete pipe. Based on the findings from the rheology test, uniaxial tensile test, centrifugal spraying test, and three-edge bearing pipe test, the following conclusions can be drawn:

- The Modified-Bingham model is more suitable than the Bingham model in depicting the nonlinear behavior between torque and shear rate of ECC or pastes developed for centrifugal spraying. Pastes without fibers exhibit a shear-thickening effect due to the addition of HPMC and metakaolin; the increased viscosity under high shear rate enhances the fiber dispersion. In contrast, aligned fiber orientations lead to a shear-thinning behavior in ECC, suggesting a decreased viscosity with increasing shear rate which facilitates the atomization of the CS-ECC into small particles under a high centrifugal spray force.
- Chemical admixtures can be utilized for engineering desirable rheological behavior of CS ECC pastes. While citric acid (retarder) has a negligible effect on the yield stress, the addition of citric acid increases the initial viscosity of paste due to the competition effect with the water reducer. Further, citric acid delays the flow loss of CS ECC/paste, extending the time window for spraying. Meanwhile, Hydroxypropyl methylcellulose (HPMC) increases both the yield stress and viscosity of ECC paste noticeably. An optimal dosage of HPMC (0.5‰ of binder weight) is shown to be advantageous for ECC layer thickness build-up.
- Fiber is the dominant factor affecting both the fresh properties and hardened properties of CS ECC. An increased viscosity or decreased spread diameter effect is established following the fiber types of PVA, PVA-PE hybrid, and PE fibers. The lowest deformability of PE ECC due to high fiber quantity limits its applicability on CS ECC. Finally, the deformability index ($D = 1.0–2.2$) is proposed as a control range for CS ECC. Although the rheological properties of PVA ECC make it more favorable for spraying, this composite shows inferior tensile performance than PE ECC and Hybrid ECC. PVA-PE hybrid ECC possesses ultra-high ductility (6.8%) and saturated cracks (91 cracks at failure). Combining both the fresh and hardening advantages, PVA-PE hybrid ECC is proposed for developing the CS ECC.
- Centrifugally sprayed ECC has been successfully demonstrated. With the deliberate design of rheology, CS ECC can build up a one-time thickness of at least 50 mm for both vertical and horizontal RC pipes. The reachable diameter (300–900 mm) meets the requirement of repairing general RC pipes, and has the potential to be further increased by air pressure/volume augmentation. The developed CS ECC attests to the advantage of no rebound due to the good adhesion and cohesion designs. Without rebound, material waste is minimized, a more uniform liner thickness is achieved, and the challenge of removing excess material in the pipe due to rebound/dripping is eliminated.
- CS ECC shows anisotropic tensile properties due to fiber alignment in the circumferential direction caused by the centrifugal spraying process. The tensile strength of 5.7 MPa and ductility of 5.3% in the circumferential direction are higher than those in the longitudinal direction (4.7 MPa and 2.2%). Although 22% of tensile ductility reduction is observed in circumferential direction compared to the mold cast specimen, the tensile ductility (5.3%) remains approximately 500 times that of conventional cementitious repair materials. Moreover, the CS ECC retains a crack width comparable to that of the mold-cast ECC.
- The superior crack control ability and ultra-high ductility of CS ECC enable structural retrofit functionality for damaged RC pipes. The CS ECC liner suppresses the brittle failure of RC pipe, exhibiting multiple microcracks in ECC liner and ductile deformation of the repaired RC pipe. Although the RC layer may eventually spall off due to the interfacial debonding between the ECC liner and the quarter-fractured host RC pipe, the ECC liner maintains a residual load-bearing capacity that remains higher than the original sound RC pipe.
- The structural improvement depends on the thickness of the sprayed CS ECC layer. A 25 mm CS ECC liner enhances the cracked RC pipe with 2.2 times of load capacity and 1.5 times of deformation capacity per ASTM C76-20. A thinner CS ECC lining with enhanced structural performance appears feasible. A thinner lining mitigates hydraulic capacity loss as well as lowers material consumption, carbon footprint, and economic cost.

Besides the retrofit superiority, CS ECC show advantages over traditional pipe rehabilitation methods, such as low cost, fast return-to-service (setting in 3 h), less surface preparation due to expansive coupling with host pipe, and flexible section shape/length range/diameter (with or without worker-entry). These characteristics render the CS ECC an attractive and promising repair technique for retrofitting concrete pipes, as well as culverts and tunnels. More factors related to the practical applications, such as the ECC curing condition, lateral confinement, and interface requirement should be considered in future studies.

Declaration of competing interest

The authors declare that they have no known competing financial interests or personal relationships that could have appeared to influence the work reported in this paper.

Acknowledgments

This research is partially supported by the James R. Rice Distinguished University Professorship of Engineering. The authors acknowledge the materials supply from BASF Chemicals company (water reducer), Entech Inc. (crumb rubber), CTS Cement Manufacturing Corporation (CSA cement), and Northern Concrete Pipe Inc. (MI, USA).

Tianyu Wang and Yichao Wang helped to conduct parts of spray tests. Their contributions are gratefully acknowledged.

References

[1] H. Zhu, T. Wang, Y. Wang, V.C. Li, Trenchless rehabilitation for concrete pipelines of water infrastructure: a review from the structural perspective, Cement Concr. Compos. 123 (2021), 104193, https://doi.org/10.1016/j.cemconcomp.2021.104193.

[2] A. Selvakumar, A.N. Tafuri, Rehabilitation of aging water infrastructure systems: key challenges and issues, J. Infrastruct. Syst. 18 (2012) 202–209, https://doi.org/10.1061/(asce)is.1943-555x.0000091.

[3] ASCE, 2021 INFRASTRUCTURE REPORT CARD, 2021. https://infrastructurereportcard.org/.

[4] H. Zhu, Y. Hu, Q. Li, R. Ma, Restrained cracking failure behavior of concrete due to temperature and shrinkage, Construct. Build. Mater. 244 (2020), https://doi.org/10.1016/j.conbuildmat.2020.118318.

[5] R. Morrison, L. Wang, State of technology report for force main rehabilitation, US Environmental Protection Agency National Risk Management Research Laboratory Water Supply and Water Resources Division, Cincinnati, 2010. https://cfpub.epa.gov/si/si_public_record_Report.cfm?Lab=NRMRL%26dirEntryID=222404.

[6] M. Najafi, Trenchless technology: Pipeline and utility design, construction, and renewal, McGraw-Hill Education, 2005. https://books.google.com/books/about/Trenchless_Technology.html?id=1rtRAAAAMAAJ.

[7] B.J. Li, L.S. Zhu, Y. Li, X.S. Fu, Experimental investigation of an existing RCP rehabilitated with a grouted corrugated steel pipe, Math. Probl Eng. 2019 (2019), https://doi.org/10.1155/2019/7676359.

[8] B.T. Huang, Q.H. Li, S.L. Xu, B. Zhou, Strengthening of reinforced concrete structure using sprayable fiber-reinforced cementitious composites with high ductility, Compos. Struct. 220 (2019) 940–952, https://doi.org/10.1016/J.COMPSTRUCT.2019.04.061.

[9] V.C. Li, Engineered Cementitious Composites (ECC), Springer, 2019, https://doi.org/10.1007/978-3-662-58438-5.

[10] H. Zhu, K. Yu, V.C. Li, Sprayable engineered cementitious composites (ECC) using calcined clay limestone cement (LC3) and PP fiber, Cement Concr. Compos. 115 (2021), 103868, https://doi.org/10.1016/j.cemconcomp.2020.103868.
[11] V.C. Li, F.P. Bos, K. Yu, W. McGee, T.Y. Ng, S.C. Figueiredo, K. Nefs, V. Mechtcherine, V.N. Nerella, J. Pan, On the emergence of 3D printable engineered, strain hardening cementitious composites (ECC/SHCC), Cement Concr. Res. 132 (2020), 106038.
[12] A.E. Bruedern, D. Abecasis, V. Mechtcherine, Development of strain-hardening cement-based composites for the strengthening of masonry, concr. Repair, rehabil. Retrofit. II, - Proc. 2nd Int. Conf. Concr. Repair, Rehabil. Retrofit. ICCRRR. (2009) 327–328, https://doi.org/10.1201/9781439828403.ch124.
[13] Z. Zhang, Q. Zhang, Self-healing ability of Engineered Cementitious Composites (ECC) under different exposure environments, Construct. Build. Mater. 156 (2017) 142–151, https://doi.org/10.1016/j.conbuildmat.2017.08.166.
[14] L.L. Kan, H.S. Shi, A.R. Sakulich, V.C. Li, Self-healing characterization of engineered cementitious composite materials, ACI Mater. J. 107 (2010) 617–624, https://doi.org/10.14359/51664049.
[15] V.C. Li, E.-H. Yang, Self healing in concrete materials, in: Self Heal. Mater., Springer, 2007, pp. 161–193.
[16] H. Zhu, D. Zhang, T. Wang, H. Wu, V.C. Li, Mechanical and self-healing behavior of low carbon engineered cementitious composites reinforced with PP-fibers, Construct. Build. Mater. 259 (2020), 119805, https://doi.org/10.1016/j.conbuildmat.2020.119805.
[17] H. Zhu, D. Zhang, T. Wang, V.C. Li, Intrinsic self-stressing and low carbon engineered cementitious composites (ECC) for improved sustainability, Cement Concr. Res. 149 (2021), 106580, https://doi.org/10.1016/j.cemconres.2021.106580.
[18] H. Zhu, D. Zhang, Y. Wang, T. Wang, V.C. Li, Development of self-stressing engineered cementitious composites (ECC), Cement Concr. Compos. 118 (2021), 103936, https://doi.org/10.1016/j.cemconcomp.2021.103936.
[19] K. Yu, W. McGee, T.Y. Ng, H. Zhu, V.C. Li, 3D-printable engineered cementitious composites (3DP-ECC): fresh and hardened properties, Cement Concr. Res. 143 (2021), 106388, https://doi.org/10.1016/j.cemconres.2021.106388.
[20] H. Zhu, K. Yu, W. McGee, T.Y. Ng, V.C. Li, Limestone calcined clay cement for three-dimensional-printed engineered cementitious composites, ACI Mater. J. 118 (2021) 111–122, https://doi.org/10.14359/51733109.
[21] Y. Zhao, B. Ma, S.T. Ariaratnam, C. Zeng, X. Yan, F. Wang, T. Wang, Z. Zhu, C. He, G. Shi, R. Mi, Structural performance of damaged rigid pipe rehabilitated by centrifugal spray on mortar liner, Tunn. Undergr. Space Technol. 116 (2021), 104117, https://doi.org/10.1016/j.tust.2021.104117.
[22] J.R. Royer, E. Allouche, Laboratory testing and analysis of geopolymer pipe-lining technology for rehabilitation of sewer & stormwater conduits, in: North Am. Soc. Trenchless Technol., NASTT's 2016 No-Dig Show, Dallas, Texas, 2016, pp. 1–10 (NASTT).
[23] D.R. Morgan, K. Loevlie, N. Kwong, A. Chan, Centrifugal placed concrete for lining horizontal pipes, culverts, and vertical shafts, Shotcrete Elem. a Syst. - Proc. 3rd Int. Conf. Eng. Dev. Shotcrete. (2010) 225–232, https://doi.org/10.1201/b10545-27.
[24] M. Li, V.C. Li, Rheology, fiber dispersion, and robust properties of engineered cementitious composites, Mater. Struct. Constr. 46 (2013) 405–420, https://doi.org/10.1617/s11527-012-9909-z.
[25] Y.Y. Kim, H.J. Kong, V.C. Li, Design of engineered cementitious composite suitable for wet-mixture shotcreting, ACI Mater. J. 100 (2003) 511–518, https://doi.org/10.14359/12958.
[26] M. Cao, W. Si, C. Xie, Relationship of rheology, fiber dispersion, and strengths of polyvinyl alcohol fiber-reinforced cementitious composites, ACI Mater. J. 117 (2020) 191–204.
[27] W. Meng, K.H. Khayat, Improving flexural performance of ultra-high-performance concrete by rheology control of suspending mortar, Compos. B Eng. 117 (2017) 26–34, https://doi.org/10.1016/J.COMPOSITESB.2017.02.019.
[28] E.H. Yang, M. Sahmaran, Y. Yang, V.C. Li, Rheological control in production of engineered cementitious composites, ACI Mater. J. 106 (2009) 357–366, https://doi.org/10.14359/56656.
[29] M. Şahmaran, Z. Bilici, E. Ozbay, T.K. Erdem, H.E. Yucel, M. Lachemi, Improving the workability and rheological properties of Engineered Cementitious Composites using factorial experimental design, Compos. B Eng. 45 (2013) 356–368, https://doi.org/10.1016/j.compositesb.2012.08.015.
[30] H. Zhu, K. Yu, V.C. Li, Citric acid influence on sprayable CSA-ECC fresh/hardened properties, ACI Mater. J. 118 (2021) 39–48, https://doi.org/10.14359/51733103.
[31] G.P.A.G. van Zijl, L. de Beer, Sprayed strain-hardening cement-based composite overlay for shear strengthening of unreinforced load-bearing masonry, Adv. Struct. Eng. 22 (2019) 1121–1135, https://doi.org/10.1177/1369433218807686.
[32] ASTM C76-20, Standard Specification for Reinforced Concrete Culvert, Storm Drain, and Sewer Pipe, ASTM International, West Conshohocken, PA, 2020, https://doi.org/10.1520/C0076-20. www.astm.org.
[33] Z. Zhang, H. Ma, S. Qian, Investigation on properties of ECC incorporating crumb rubber of different sizes, J. Adv. Concr. Technol. 13 (2015) 241–251, https://doi.org/10.3151/jact.13.241.
[34] J.S. Kim, J.K. Kim, G.J. Ha, Y.Y. Kim, Rheological control of cement paste for applying prepackaged ECCS (engineered cementitious composites) to self-consolidating and shotcreting processes, KSCE J. Civ. Eng. 14 (2010) 743–751, https://doi.org/10.1007/s12205-010-0796-y.
[35] K.Q. Yu, J.T. Yu, J.G. Dai, Z.D. Lu, S.P. Shah, Development of ultra-high performance engineered cementitious composites using polyethylene (PE) fibers, Construct. Build. Mater. 158 (2018) 217–227, https://doi.org/10.1016/J.CONBUILDMAT.2017.10.040.
[36] ASTM C1437-15, Standard Test Method for Flow of Hydraulic Cement Mortar, ASTM International, West Conshohocken, PA, 2015. www.astm.org.
[37] D. Feys, J.E. Wallevik, A. Yahia, K.H. Khayat, O.H. Wallevik, Extension of the Reiner-Riwlin equation to determine modified Bingham parameters measured in coaxial cylinders rheometers, Mater. Struct. Constr. 46 (2013) 289–311, https://doi.org/10.1617/s11527-012-9902-6.
[38] A. Selvakumar, A.N. Tafuri, R. Morrison, R. Sterling, State of technology for renewal of sewer force mains, Urban Water J. 8 (2011) 279–292, https://doi.org/10.1080/1573062X.2011.598171.
[39] ASTM C497M-19, Standard Test Methods for Concrete Pipe, Concrete Box Sections, Manhole Sections, or Tile (Metric), ASTM International, West Conshohocken, PA, 2019, https://doi.org/10.1520/C0497M-19. www.astm.org.
[40] D. Feys, R. Verhoeven, G. De Schutter, Why is fresh self-compacting concrete shear thickening? Cement Concr. Res. 39 (2009) 510–523, https://doi.org/10.1016/j.cemconres.2009.03.004.
[41] M. Cyr, C. Legrand, M. Mouret, Study of the shear thickening effect of superplasticizers on the rheological behaviour of cement pastes containing or not mineral additives, Cement Concr. Res. 30 (2000) 1477–1483, https://doi.org/10.1016/S0008-8846(00)00330-6.
[42] A. Yahia, Effect of solid concentration and shear rate on shear-thickening response of high-performance cement suspensions, Construct. Build. Mater. 53 (2014) 517–521, https://doi.org/10.1016/j.conbuildmat.2013.10.078.
[43] R.L. Hoffman, Explanations for the cause of shear thickening in concentrated colloidal suspensions, J. Rheol. 42 (1998) 111–123, https://doi.org/10.1122/1.550884.
[44] C. Liu, X. Wang, Y. Chen, C. Zhang, L. Ma, Z. Deng, C. Chen, Y. Zhang, J. Pan, N. Banthia, Influence of hydroxypropyl methylcellulose and silica fume on stability, rheological properties, and printability of 3D printing foam concrete, Cement Concr. Compos. 122 (2021), 104158, https://doi.org/10.1016/J.CEMCONCOMP.2021.104158.
[45] P. Coussot, Introduction to the rheology of complex fluids, Underst. Rheol. Concr. (2012) 3–22, https://doi.org/10.1533/9780857095282.1.3.
[46] S. Grünewald, Fibre reinforcement and the rheology of concrete, in: N. Roussel (Ed.), Underst. Rheol. Concr., Woodhead Publishing, 2012, pp. 229–256, https://doi.org/10.1533/9780857095282.2.229.
[47] K.H. Khayat, N. Mikanovic, Viscosity-enhancing admixtures and the rheology of concrete, Underst. Rheol. Concr. (2012) 209–228, https://doi.org/10.1533/9780857095282.2.209.
[48] B. Ma, Y. Peng, H. Tan, S. Jian, Z. Zhi, Y. Guo, H. Qi, T. Zhang, X. He, Effect of hydroxypropyl-methyl cellulose ether on rheology of cement paste plasticized by polycarboxylate superplasticizer, Construct. Build. Mater. 160 (2018) 341–350, https://doi.org/10.1016/J.CONBUILDMAT.2017.11.010.
[49] K.H. Khayat, W. Meng, K. Vallurupalli, L. Teng, Rheological properties of ultra-high-performance concrete — an overview, Cement Concr. Res. 124 (2019), 105828, https://doi.org/10.1016/J.CEMCONRES.2019.105828.
[50] H.J. Kong, S.G. Bike, V.C. Li, Constitutive rheological control to develop a self-consolidating engineered cementitious composite reinforced with hydrophilic poly (vinyl alcohol) fibers, Cement Concr. Compos. 25 (2003) 333–341, https://doi.org/10.1016/S0958-9465(02)00056-2.
[51] S. Chaves Figueiredo, O. Çopuroğlu, E. Schlangen, Effect of viscosity modifier admixture on Portland cement paste hydration and microstructure, Construct. Build. Mater. 212 (2019) 818–840, https://doi.org/10.1016/J.CONBUILDMAT.2019.04.020.
[52] G. Ke, J. Zhang, Effects of retarding admixture, superplasticizer and supplementary cementitious material on the rheology and mechanical properties of high strength calcium sulfoaluminate cement paste, J. Adv. Concr. Technol. 18 (2020) 17–26, https://doi.org/10.3151/jact.18.17.
[53] B. Rachid, G. Philippe, G. Alexandre, Hydration and rheology of sulfoaluminate cements (CSA) in presence of polycarboxylate superplasticizers (PCE) and citric acid, in: 5th International Congress on the Chemistry of Cement a success (ICCC 2019), Research Institute of Binding Materials Prague Ltd., 2019. https://hal.archives-ouvertes.fr/hal-02360076/.
[54] K. Zhang, L. Pan, J. Li, C. Lin, What is the mechanism of the fiber effect on the rheological behavior of cement paste with polycarboxylate superplasticizer? Construct. Build. Mater. 281 (2021), 122542 https://doi.org/10.1016/J.CONBUILDMAT.2021.122542.
[55] E. Secrieru, V. Mechtcherine, C. Schröfl, D. Borin, Rheological characterisation and prediction of pumpability of strain-hardening cement-based-composites (SHCC) with and without addition of superabsorbent polymers (SAP) at various temperatures, Construct. Build. Mater. 112 (2016) 581–594, https://doi.org/10.1016/j.conbuildmat.2016.02.161.
[56] K. Yu, W. Mcgee, T. Yan, H. Zhu, V.C. Li, Cement and Concrete Research 3D-printable engineered cementitious composites (3DP-ECC): fresh and hardened properties, Cement Concr. Res. 143 (2021), 106388, https://doi.org/10.1016/j.cemconres.2021.106388.
[57] Y. Zhu, Z. Zhang, Y. Yao, X. Guan, Y. Yang, Effect of water-curing time on the mechanical properties of engineered cementitious composites, J. Mater. Civ. Eng. 28 (2016), 04016123, https://doi.org/10.1061/(asce)mt.1943-5533.0001636.
[58] X. Wang, Understanding the Placement Mechanism of Wet-Mix Shotcrete and the Influence of Material Properties, Florida State University, 2021.
[59] J. Kaufmann, K. Frech, P. Schuetz, B. Münch, Rebound and orientation of fibers in wet sprayed concrete applications, Construct. Build. Mater. 49 (2013) 15–22, https://doi.org/10.1016/j.conbuildmat.2013.07.051.
[60] K.Q. Yu, W.J. Zhu, Y. Ding, Z.D. Lu, J. tao Yu, J.Z. Xiao, Micro-structural and mechanical properties of ultra-high performance engineered cementitious

composites (UHP-ECC) incorporation of recycled fine powder (RFP), Cem, Concr. Res. 124 (2019), 105813, https://doi.org/10.1016/j.cemconres.2019.105813.
[61] R. Ranade, Advanced Cementitious Composite Development for Resilient and Sustainable Infrastructure, University of Michigan, 2014.
[62] Y.M. Lim, V.C. Li, Durable repair of aged infrastructures using trapping mechanism of engineered cementitious composites, Cement Concr. Compos. 19 (1997) 373–385, https://doi.org/10.1016/S0958-9465(97)00026-7.
[63] T. Kamada, V.C. Li, The effects of surface preparation on the fracture behavior of ECC/concrete repair system, Cement Concr. Compos. 22 (2000) 423–431, https://doi.org/10.1016/S0958-9465(00)00042-1.
[64] J. Wang, D. Niu, Y. Zhang, Mechanical properties, permeability and durability of accelerated shotcrete, Construct. Build. Mater. 95 (2015) 312–328, https://doi.org/10.1016/J.CONBUILDMAT.2015.07.148.